

Scheme Independence to all Loops

Oliver J. Rosten

School of Physics and Astronomy, University of Southampton, Highfield,
Southampton SO17 1BJ, U.K.

E-mail: O.J.Rosten@soton.ac.uk

Abstract. The immense freedom in the construction of Exact Renormalization Groups means that the many non-universal details of the formalism need never be exactly specified, instead satisfying only general constraints. In the context of a manifestly gauge invariant Exact Renormalization Group for $SU(N)$ Yang-Mills, we outline a proof that, to all orders in perturbation theory, all explicit dependence of β function coefficients on both the seed action and details of the covariantization cancels out. Further, we speculate that, within the infinite number of renormalization schemes implicit within our approach, the perturbative β function depends only on the universal details of the setup, to all orders.

PACS numbers: 11.10.Gh, 11.15.-q, 11.10.Hi

1. Introduction and Conclusions

The Exact Renormalization Group (ERG) provides an extremely flexible framework for dealing with Quantum Field Theory, as a direct consequence of the immense freedom in its actual construction [1, 2]. Remarkably, this freedom can be exploited to construct ERGs for $SU(N)$ Yang-Mills theory in which the gauge invariance is *manifestly* preserved [2–10], with the realization of a gauge invariant cutoff being achieved by embedding the physical theory, carried by the field A_μ^1 , in a spontaneously broken $SU(N|N)$ gauge theory [11]. In addition to the coupling, g , of the physical gauge field, there is a second running, dimensionless coupling, g_2 , associated with one of the unphysical regulator fields, A_μ^2 . As a consequence of g and g_2 renormalizing separately, it is convenient to further specialize to those ERGs which treat A_μ^1 and A_μ^2 asymmetrically, in the broken phase [2, 8]. The resulting formalism has been used to successfully compute the $SU(N)$ Yang-Mills two-loop β function, β_2 [2, 8–10], without fixing the gauge.

Despite the restrictions we choose to impose on the ERG, there are still an infinite number with which we can work, corresponding to the residual freedom in the precise details of the construction; and this residual freedom, too, can be turned to our advantage. The differences between the admissible ERGs amount to non-universal details which, whilst encoding the ultra-violet regularization, parameterize the continuum notion of a general Kadanoff blocking procedure [1, 2]. Our philosophy is to leave the non-universal details largely unspecified, defining them implicitly where necessary, to ensure that the flow equation is well behaved. As a direct consequence, the computation of universal quantities becomes particularly efficient. A universal quantity cannot depend on non-universal details; by leaving these details essentially unspecified, their cancellation becomes so constrained that it can be performed diagrammatically. In other words, the diagrammatics represent the natural way of encoding the non-universalities inherent in the flow equation.

These observations underpin the computation of the universal coefficient β_2 , in which diagrammatic techniques are used to iteratively remove non-universal contributions. To elucidate this procedure, we enumerate the various sources of non-universality. First, there is the precise form of the cutoff functions. Secondly, there are the details of the covariantization of the cutoff. Lastly, there is the ‘seed action’, \hat{S} [2, 6, 8, 10, 12–14]: a functional which respects the same symmetries as the Wilsonian effective action, S , and has the same structure. However, whereas our aim is to solve the flow equation for S , \hat{S} acts as an input.

The reduction of β_2 to an expression manifestly independent of non-universal details is a two-step procedure. First, all explicit dependence on the seed action and details of the covariantization is removed. Secondly, all implicit dependence on these objects and all dependence on the shapes of the cutoff profiles is either cancelled or shown to vanish in an appropriate limit [8, 10].

As recognized in [8, 9], the first diagrammatic step can in fact be employed at any number of loops. This is, in some respects, quite surprising. Between certain classes of

renormalization schemes, one expects agreement only between the first two β function coefficients [6, 15]. Thus, there is no *a priori* reason to expect that, within the infinite number of renormalization schemes implicitly defined by our approach, entire sources of non-universality will cancel out in the computation of β function coefficients, to all orders in perturbation theory.

It is now natural to speculate whether the second diagrammatic step—which, like the first, is algorithmic—can be employed at any number of loops. There are encouraging indications that this is indeed the case [17]. Hence, we are led to speculate whether the β function coefficients computed in this approach could depend only on the universal details of the setup, to all orders in perturbation theory. It should be emphasised that this is not a speculation that the β function is universal in a general sense, since agreement would certainly not be expected between this ERG scheme and, say, dimensional regularization for $\beta_{n>2}$. Rather, the β function may be universal in a restricted sense: if one were to imagine the complete space of renormalization schemes, then the schemes defined by our approach would correspond to a ‘flat direction’[‡] in the sense that, when traversed, the β -function coefficients would remain unchanged, to all orders in perturbation theory.

Irrespective of whether or not universality in this restricted sense is found, the reduction of β function coefficients to a form independent of the explicit details of the seed action and details of the covariantization is of interest in itself. Furthermore, we note that since this reduction is a feature of the structure of the flow equation itself, rather than some specific feature relating to the non-Abelian gauge invariance, this analysis should be trivially extendable to scalar field theory and QED.

At this point, it is worth noting that there have been many other ERG computations of one and two loop β functions, in a variety of different theories and for a variety of different reasons [12, 13, 18–24]. The emphasis of this paper is complete scheme independence, inspired by the algorithmic removal of non-universal elements, order by order in perturbation theory. Indeed, this procedure allows us to derive an extremely compact diagrammatic formula for arbitrary β_n in terms of a set of objects (about which we will be more precise shortly) with no explicit dependence on the seed action or details of the covariantization.

The discovery of this formula is an extremely important step in promoting the ERG advocated by this paper into a practical computational scheme, as it represents a radical simplification of loop calculations. Since its inspiration comes simply from the idea that non-universal objects must cancel out in the computation of universal quantities, it is reasonable to hope that similar simplifications will be found in more general computations. Specifically, for Yang-Mills theory, we plan to compute expectation values of gauge invariant operators [17]. An exciting possibility is that this could guide us to a more direct framework for performing manifestly gauge invariant computations, where objects such as the seed action would operate entirely in the background. Indeed, it

[‡] I would like to thank Daniel Litim for pointing out this interpretation.

may be able to go further and use the current scheme as inspiration for a manifestly gauge invariant formalism entirely independent of the ERG, in which universality is transparent, from the start. We leave the investigation of these issues for the future [17].

At the heart of the diagrammatic techniques is the ‘effective propagator relation’ [6]. It is technically useful to set the two-point, tree level seed action vertices equal to their Wilsonian effective action counterparts. In turn, this ensures that for each independent two-point, tree level vertex (that cannot be consistently set to zero [8]) there exists an ‘effective propagator’, denoted by Δ , which is the inverse of the given vertex, up to a ‘gauge remainder’. This remainder term appears as a consequence of the manifest gauge invariance: the effective propagators are inverses of the two-point, tree level vertices only in the transverse space. The effective propagator relation is of such central importance since it allows the simplification of any diagram in which a two-point vertex attaches to an effective propagator. The resulting contributions are involved in direct diagrammatic cancellations, up to remainders which can themselves be processed, diagrammatically.

We now review the iterative diagrammatic procedure employed in the first phase of the calculation of β_2 [8, 9], as a precursor to discussing the computation of arbitrary β_n . To begin, the flow equation is used to compute the flow of the two-point vertex corresponding to the physical $SU(N)$ gauge field, which we suppose carries momentum p . To obtain a solvable equation for β_2 , we specialize to the appropriate loop order and work at $\mathcal{O}(p^2)$; this latter step constrains the equation by allowing the renormalization condition for the physical coupling $g(\Lambda)$ to feed in.

We now recognize that certain diagrams generated by the flow comprise exclusively Wilsonian effective action vertices joined together by $\overset{\bullet}{\Delta}$ where, having defined

$$\alpha \equiv \frac{g_2^2}{g^2}, \tag{1}$$

we define

$$\overset{\bullet}{X} \equiv -\Lambda \partial_\Lambda |_\alpha X; \tag{2}$$

$\Lambda \partial_\Lambda$ being the generator of the ERG flow. The manipulable diagrams are processed by moving $\Lambda \partial_\Lambda |_\alpha$ from the effective propagator to strike the diagram as a whole, minus correction terms in which $\Lambda \partial_\Lambda |_\alpha$ strikes the vertices. The former terms are called Λ -derivative terms; the latter terms can be processed using the flow equation and the resulting set of diagrams simplified and further processed, using a set of diagrammatic identities, of which the effective propagator relation is one [9]. At this point, we are able to identify cancellations of non-universal contributions. Iterating the diagrammatic procedure, the expression for β_2 ultimately reduces to the following sets of diagrams:

- (i) Λ -derivative terms;
- (ii) ‘ α -terms’, consisting of diagrams containing a component struck by $\partial/\partial\alpha$;
- (iii) ‘ $\mathcal{O}(p^2)$ -terms’, which contain an $\mathcal{O}(p^2)$ stub i.e. a diagrammatic component which is manifestly $\mathcal{O}(p^2)$.

In turn, the $\mathcal{O}(p^2)$ terms can be diagrammatically manipulated, thereby reducing the entire expression for β_2 to a set of Λ -derivative terms and a set of α -terms. All these diagrams contain only Wilsonian effective action vertices, effective propagators and (components of) gauge remainders.

At arbitrary loop order, precisely the same procedure can be employed [8]. However, if the answer is known, it is much more efficient to essentially take this as the starting point and prove it to be true. The precise strategy is to construct a set of terms, \mathcal{D}_n , including β_n , which vanishes at $\mathcal{O}(p^2)$. Then, at $\mathcal{O}(p^2)$, \mathcal{D}_n can be rearranged to give a compact expression for β_n in terms of just Wilsonian effective action vertices, effective propagators and (components of) gauge remainders. After giving the diagrammatic form for the flow equation in section 2, in section 3 we partially construct \mathcal{D}_n and sketch the proof that it does indeed vanish, as required (both the full expression for \mathcal{D}_n and the complete proof that it vanishes at $\mathcal{O}(p^2)$ will be given in [16]).

2. The Flow Equation

The diagrammatic representation of the flow equation is shown in figure 1 [2, 8].

$$\begin{aligned}
 -\Lambda\partial_\Lambda \left[\textcircled{S} \right]^{\{f\}} &= a_0[S, \Sigma_g]^{\{f\}} - a_1[\Sigma_g]^{\{f\}} \\
 &= \frac{1}{2} \left[\begin{array}{c} \textcircled{\Sigma_g} \\ \bullet \\ \textcircled{S} \end{array} - \textcircled{\Sigma_g} \right]^{\{f\}}
 \end{aligned}$$

Figure 1. The diagrammatic form of the flow equation.

The left-hand side depicts the flow of all independent Wilsonian effective action vertex *coefficient functions*, which correspond to the set of broken phase fields, $\{f\}$. Each coefficient function has associated with it an implied supertrace structure (and symmetry factor which, as one would want, does not appear in the diagrammatics), as expected from the embedding of the physical gauge field into a spontaneously broken $SU(N|N)$ theory [11]. For example,

$$\left[\textcircled{S} \right]^{A^1 A^1 A^1 A^1}$$

represents both the coefficient functions $S^{A^1 A^1 A^1 A^1}$ and $S^{A^1 A^1, A^1 A^1}$ which, respectively, are associated with the supertrace structures $\text{str } A^1 A^1 A^1 A^1$ and $\text{str } A^1 A^1 \text{str } A^1 A^1$ (there are no further coefficient functions / supertrace structures associated with the vertex since $\text{str } A^1 = 0$).

The dumbbell-like diagram on the right-hand side of figure 1 is formed by the bilinear functional $a_0[S, \Sigma_g]$, whereas the padlock-like diagram is formed by $a_1[\Sigma_g]$. (a_1

can also generate a diagram in which the kernel ‘bites its own tail’ [3]. Such diagrams are improperly UV regularized and can be removed by an appropriate constraint on the covariantization [2, 6].) Both diagrams comprise two different components. The lobes represent vertices of action functionals, where $\Sigma_g \equiv g^2 S - 2\hat{S}$. The object attaching to the various lobes, $\text{---}\bullet\text{---}$, is the sum over vertices of the covariantised ERG kernels [4, 6] and, like the action vertices, can be decorated by fields belonging to $\{f\}$. The fields of the action vertex (vertices) to which the vertices of the kernels attach act as labels for the ERG kernels [2, 8]. We loosely refer to both individual and summed over vertices of the kernels simply as a kernel. The rule for decorating the diagrams on the right-hand side is simple: the set of fields, $\{f\}$, are distributed in all independent ways between the component objects of each diagram. We will see an example of this in the next section.

2.1. The Weak Coupling Expansion

In the perturbative domain, we have the following weak coupling expansions [2, 8]. The Wilsonian effective action is given by

$$S = \sum_{i=0}^{\infty} (g^2)^{i-1} S_i = \frac{1}{g^2} S_0 + S_1 + \dots, \quad (3)$$

where S_0 is the classical effective action and the $S_{i>0}$ the i th-loop corrections. The seed action has a similar expansion:

$$\hat{S} = \sum_{i=0}^{\infty} g^{2i} \hat{S}_i. \quad (4)$$

The β function is defined, as usual, to be

$$\beta \equiv \Lambda \partial_{\Lambda} g = \sum_{i=1}^{\infty} g^{2i+1} \beta_i(\alpha) \quad (5)$$

where we note that $\beta_{n>1}$ are expected to depend on α . Indeed, this is true even at two-loops, where the universal coefficient is recovered only in the limit that $\alpha \rightarrow 0$ [2, 8, 10]. Should it be possible to introduce a notion of a universal β function, in the sense outlined earlier, this would presumably require that α be tuned to zero, order by order. The flow of α itself has the following expansion:

$$\gamma \equiv \Lambda \partial_{\Lambda} \alpha = \sum_{i=1}^{\infty} g^{2i} \gamma_i(\alpha). \quad (6)$$

Taking the supergauge field into which A_{μ}^1 and A_{μ}^2 are embedded to be \mathcal{A}_{μ} , and working in the broken phase, the couplings g and α are defined through their renormalization conditions:

$$S[\mathcal{A} = A^1] = \frac{1}{2g^2} \text{str} \int d^D x (F_{\mu\nu}^1)^2 + \dots, \quad (7)$$

$$S[\mathcal{A} = A^2] = \frac{1}{2\alpha g^2} \text{str} \int d^D x (F_{\mu\nu}^2)^2 + \dots, \quad (8)$$

where the ellipses stand for higher dimension operators and the ignored vacuum energy. Note that the renormalization condition for g constrains the two-point vertex of the physical field $S_{\mu}^{A^1 A^1}(p)$ as follows:

$$S_{0\mu\nu}^{11}(p) = 2(p^2\delta_{\mu\nu} - p_\mu p_\nu) + \mathcal{O}(p^4) \quad (9)$$

$$S_{n>0\mu\nu}^{11}(p) = \mathcal{O}(p^4), \quad (10)$$

where we abbreviate A^1 by just ‘1’.

Defining $\Sigma_i = S_i - 2\hat{S}_i$, the weak coupling flow equations follow from substituting (3)–(6) into the flow equation, as shown in figure 2 [2, 8].

$$\left[\begin{array}{c} \bullet \\ \circ \\ n \end{array} \right]^{\{f\}} = \left[\begin{array}{c} \sum_{r=1}^n \left[2(n_r - 1)\beta_r + \gamma_r \frac{\partial}{\partial \alpha} \right] \begin{array}{c} \circ \\ n_r \end{array} \\ + \frac{1}{2} \left(\sum_{r=0}^n \begin{array}{c} \begin{array}{c} \circ \\ \bar{n}_r \end{array} \\ \bullet \\ \begin{array}{c} \circ \\ \bar{r} \end{array} \end{array} - \begin{array}{c} \bullet \\ \circ \\ \Sigma_{n-} \end{array} \right) \end{array} \right]^{\{f\}} \quad (11)$$

Figure 2. The weak coupling flow equations.

We refer to the first two terms on the right-hand side of (11) as β and α -terms, respectively. The symbol \bullet , as in equation (2), means $-\Lambda\partial_\Lambda|_\alpha$. A vertex whose argument is an unadorned letter, say n , represents S_n . We define $n_r \equiv n - r$ and $n_\pm = n \pm 1$. The bar notation of the dumbbell term is defined as follows:

$$a_0[\bar{S}_{n-r}, \bar{S}_r] \equiv a_0[S_{n-r}, S_r] - a_0[S_{n-r}, \hat{S}_r] - a_0[\hat{S}_{n-r}, S_r]. \quad (12)$$

The effective propagator relation [6] is central to the perturbative diagrammatic approach, and arises from examining the flow of all two-point, tree level vertices. This is done by setting $n = 0$ in (11) and specialising $\{f\}$ to contain two fields, as shown in figure 3. We note that we can and do choose all such vertices to be single supertrace terms [2, 8].

$$\begin{array}{c} \bullet \\ \circ \\ 0 \end{array} = \begin{array}{c} \circ \\ 0 \end{array} \bullet - \begin{array}{c} \hat{\circ} \\ \bullet \\ \circ \\ 0 \end{array} - \begin{array}{c} \circ \\ 0 \end{array} \bullet - \begin{array}{c} \circ \\ \bullet \\ \hat{\circ} \end{array} \quad (13)$$

Figure 3. Flow of all possible two-point, tree level vertices.

Following [2–6, 8, 13] we use the freedom inherent in \hat{S} by choosing the two-point, tree level seed action vertices equal to the corresponding Wilsonian effective action vertices. Equation (13) now simplifies. Rearranging, integrating with respect to Λ

and choosing the appropriate integration constants [2, 8], we arrive at the relationship between the integrated ERG kernels—a.k.a. the effective propagators—and the two-point, tree level vertices shown in figure 4. Note that we have attached the effective propagator, which only ever appears as an internal line, to an arbitrary structure.

$$\begin{aligned}
 M \text{---} \textcircled{0} \text{---} \langle \rangle &\equiv M \text{---} \langle \rangle - M \blacktriangleright \langle \rangle \\
 &\equiv M \text{---} \langle \rangle - M \triangleright \triangleright \langle \rangle
 \end{aligned}$$

Figure 4. The effective propagator relation.

The field labelled by M can be any of the broken phase fields. The first term on the right-hand side is the Kronecker- δ part of the effective propagator relation, and the second term is the gauge remainder part. The gauge remainder decomposes into two separate components, \triangleright and \triangleright , as indicated on the second line. These individual components will often be loosely referred to as gauge remainders (see [2, 8, 9] for far more detail).

We conclude this section by introducing some new notation. First, we introduce a set of vertex arguments, v^j , where the upper roman index acts as a label. Thus, the v^j are integers, denoting the loop orders of some set of vertices. Given that both the vertex arguments and number of legs of the vertices we will shortly encounter are to be summed over, it is useful to introduce reduced vertices, defined not to possess a two-point, tree level component. This is denoted by appending the appropriate vertex argument with a superscript R , viz $v^{j;R}$.

Next, we introduce the compact notation

$$\begin{aligned}
 v^{j,j+} &\equiv v^j - v^{j+1} \\
 v^{j,j+;R} &\equiv v^{j;R} - v^{j+1;R}.
 \end{aligned}$$

We use this notation to define

$$\textcircled{n_s, j} \equiv \prod_{i=0}^j \sum_{v^{i+}=0}^{v^i} \textcircled{v^{i,i+;R}}, \quad (14)$$

where the first argument of the structure on the left-hand side, n_s , gives the value of v^0 . Notice that all other vertex arguments are summed over. The interpretation of the product symbol is as a generator of $j + 1$ vertices.

The structure shown in (14) always appears as a part of diagrams which possess an additional vertex, which carries the argument v^{j+} (this argument need not appear on its own—it could be part of something more complicated e.g. $v^{j+,k}$). An example,

which will play an important role later, is

$$\left[\begin{array}{c} \textcircled{v^{j+;R}} \\ \textcircled{n_s, j} \end{array} \right] \equiv \prod_{i=0}^j \sum_{v^{i+}=0}^{v^i} \left[\begin{array}{c} \textcircled{v^{j+;R}} \\ \textcircled{v^{i,i+;R}} \end{array} \right]. \quad (15)$$

Notice that the sum over all vertex arguments is trivially n_s :

$$\sum_{i=0}^j v^{i,i+} + v^{j+} = \sum_{i=0}^j (v^i - v^{i+1}) + v^{j+1} = v^0 = n_s. \quad (16)$$

The interpretation that the structure defined by (14) possesses $j+1$ vertices allows us to usefully define (15) for $j = -1$:

$$\left[\begin{array}{c} \textcircled{v^{j+;R}} \\ \textcircled{n_s, j} \end{array} \right]_{j=-1} \equiv \textcircled{n_s^R}, \quad (17)$$

where n_s^R is, of course, just an $n-s$ -loop, reduced vertex. (Note that this example illustrates the rule that v^{j+} is replaced by n ; this holds irrespective of whether or not v^{j+} occurs only as part of some more complicated vertex argument.) We can even usefully define what we mean by (15) for $j = -2$:

$$\left[\begin{array}{c} \textcircled{v^{j+;R}} \\ \textcircled{n_s, j} \end{array} \right]_{j=-2} \equiv \delta(n-s). \quad (18)$$

Notice that (17) still makes sense if one and only one of the vertices is decorated (in practise, we will always take this to be the top vertex): if more than one vertex is decorated then this implies that the number of vertices is at least two, which leads to a contradiction. On the other hand, (18) makes sense only as is, and not if any of the vertices are decorated. In the computation of β_n , we will find structures like (15), where we sum over j . The lower value of this sum will start out at -2 . However, as we perform explicit decorations of the vertices, so we will need to raise the lower limit on j , such that the diagrams still make sense.

The notation introduced above will allow us to conveniently represent the vertices of diagrams contributing to β_n . However, diagrams contain three additional ingredients: external fields, effective propagators and gauge remainder components. We now introduce notation and rules for these objects, in a manner compatible with our diagrammatics for the vertices.

To this end, consider the diagrammatic expression shown in figure 5.

The diagrams represented in figure 5 possess the following:

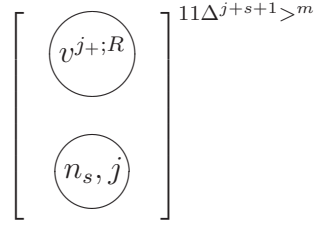


Figure 5. Representation of a set of diagrams in terms of vertices, external fields, effective propagators and gauge remainders.

- (i) $j + 2$ reduced vertices;
- (ii) two external physical gauge fields, each denoted by ‘1’ (Lorentz indices are henceforth suppressed);
- (iii) $j + s + 1$ effective propagators;
- (iv) m gauge remainder components, $>$.

The gauge remainder components behave, diagrammatically, in a similar manner to the vertices, in that they form structures which must be attached to other structures via internal lines. In this paper, we will not go into detail about the structures that the gauge remainders can form (see [8, 16] for more detail); rather, we note the following. First, each gauge remainder possesses a ‘socket’ which must be filled by either an external field or one end of an effective propagator i.e. \longrightarrow . Secondly, suppose that we wish to partition m gauge remainders into two groups of m' and $m - m'$, which form separate structures. The combinatoric factor associated with this division is just ${}^{m'}C_m$, reflecting the indistinguishability of the m gauge remainders.

Next, we focus on the effective propagators. Suppose that we wish to join together two vertices with q effective propagators. First, we note that each of the $j + 2$ vertices is equivalent (before decoration), as can be straightforwardly checked by a change of variables. Hence, there are ${}^{j+2}C_2$ different pairs of vertices we can chose. Now, we must partition the effective propagators into two sets containing q and $j + s + 1 - q$ elements. There are ${}^{j+s+1}C_q$ ways to do this. Finally, we note that each effective propagator can attach with either end to either vertex, yielding a further factor of 2^q . Thus, referring to figure 5, there are

$$2^q \times {}^{j+2}C_2 \times {}^{j+s+1}C_q$$

ways of joining a pair of vertices together with q effective propagators. Effective propagators need not join one object to another but can instead form loops on vertices. In this case, since the ends of such an effective propagator attach to the same structure, no factor of two arises from the indistinguishability of the two ends.

Finally, we can decorate structures with the two external fields. If the two external fields both attach to the same vertex, then the combinatoric factor is just unity. If each of the external fields attaches to a different object then there is an associated combinatoric factor of two, arising from the indistinguishability of the two external fields.

The rule for generating the set of fully fleshed out diagrams represented in figure 5 is simple. First, we form all possible combinations of gauge remainder structures. Next, we decorate both the gauge remainder structures and vertices with the effective propagators and external fields in all possible ways, ensuring that there are no empty sockets and that all diagrams are connected. The combinatorics follows intuitively from the indistinguishability of the elements of each set of diagrammatic components from the other elements in the same set.

3. An Expression for β_n

An expression for β_n in terms of just Wilsonian effective action vertices, effective propagators and gauge remainders can be derived by demonstrating that the set of diagrams shown in figure 6, \mathcal{D}_n , whose external momentum we take to be p , vanishes at $\mathcal{O}(p^2)$.

$$\begin{aligned}
\mathcal{D}_n = & \mathcal{D}'_n + 2 \sum_{s=0}^n \sum_{m=0}^{2s+1} \sum_{j=-2}^{n+s-m-1} \frac{\Upsilon_{j+s+1,j+2}}{m!} \left[\left[\begin{array}{c} \textcircled{v^{j+};R} \\ \textcircled{n_s, j} \end{array} \right]^{11\Delta^{j+s+1} > m} \right]^\bullet \\
& + 2 \sum_{s=0}^n \sum_{m=0}^{2s} \sum_{j=-1}^{n+s-m-2} \frac{\Upsilon_{j+s+1,j+1}}{m!} \\
& \times \sum_{v^k=1}^{v^{j+}} \left[\begin{array}{c} \left[2(v^{j+,k} - 1) \beta_{v^k} + \gamma_{v^k} \frac{\partial}{\partial \alpha} \right] \textcircled{v^{j+,k}} \\ \textcircled{n_s, j} \end{array} \right] \quad (19)
\end{aligned}$$

Figure 6. A set of diagrams which vanishes at $\mathcal{O}(p^2)$.

\mathcal{D}_n represents a set of Λ -derivative, β and α -terms possessing an $\mathcal{O}(p^2)$ stub; we defer giving an explicit expression for \mathcal{D}'_n until [16]. For the non-negative integers a and b , we define

$$\Upsilon_{a,b} = \frac{(-1)^{b+1}}{a!b!} \left(\frac{1}{2}\right)^{a+1}; \quad (20)$$

if either a or b is negative, the function is null.

Before moving on, a comment is in order concerning the ranges of the various summations in figure 6. We begin by focusing on the Λ -derivative term. The value of s controls the sum of the vertex arguments and thus the maximum loop order vertex that can appear. If s takes its maximum value of n , then the sum over the vertex arguments is zero: all vertices are tree level. At the other extreme, the sum over the

vertex arguments is n , and so it is clear that the maximum loop order vertex that can appear is n , as one would expect.

The maximum values of the sums over m and j follow from the rule that all fully fleshed out diagrams must be connected. Of the $j + 2$ vertices, suppose that T are tree level vertices. Since the vertices are reduced (meaning that the tree level vertices cannot have precisely two decorations), and one-point tree level vertices are automatically zero, a minimum of $3T$ decorations are required for the tree level vertices. What of the remaining $j + 2 - T$ vertices? It is imposed as a constraint that all one-point, Wilsonian effective action vertices vanish[§], in order that the vacuum expectation value of the superscalar which breaks the $SU(N|N)$ symmetry is not shifted by quantum corrections [6]. This requirement manifests itself as a constraint on the seed action. We can thus insist that all Wilsonian effective action vertices are at least two-point. However, it is technically convenient to allow the diagrams of figure 6 to possess a single one-point vertex. If this vertex is struck by $-\Lambda\partial_\Lambda|_\alpha$ then it generates a set of diagrams, not all of which vanish individually. Using the flow equation to re-express zero in this way essentially enforces the aforementioned constraint on the seed action ‘on the fly’. Hence, we use the following prescription: we allow a single one-point, Wilsonian effective action vertex *before* the action of $-\Lambda\partial_\Lambda|_\alpha$. After $-\Lambda\partial_\Lambda|_\alpha$ has acted, we adjust the ranges on the sums, as appropriate, to ensure that no one-point, Wilsonian effective action vertices remain.

Given T tree level vertices, at most one one-point vertex, and m gauge remainders, we require a minimum of

$$2(j + 1 - T) + 3T + 1 + m = 2j + T + m + 3 \quad (21)$$

decorations. Recalling that effective propagators are two-ended objects and that we have two external fields, we see that there are

$$2(j + s + 1) + 2$$

available decorations. It is thus clear that

$$T + m \leq 2s + 1. \quad (22)$$

It therefore follows that

$$m \leq 2s + 1. \quad (23)$$

Next, let us deduce the maximum number of vertices i.e. the maximum number taken by $j + 2$ for some values of s and m . From (16), we know that the sum over vertex arguments is $n - s$. Therefore, we can have at most $n - s$ vertices which are not tree level and so a total of $n - s + T$ vertices. Hence,

$$j + 2 \leq n + s - m + 1,$$

where we have used (22).

[§] One-point, *seed* action vertices do exist, beyond tree level.

The ranges on the sums for the α and β terms follow similarly but now we explicitly remove any diagrams with one-point vertices (since they cannot be processed) by lowering the upper limits on the sums over m and j by one apiece. Furthermore, the lower limit of the sum over j is -1 and not -2 , since there must be at least one vertex present.

Having justified the ranges on the various sums, we proceed by simply allowing $-\Lambda\partial_\Lambda|_\alpha$ to act. In the case where $-\Lambda\partial_\Lambda|_\alpha$ strikes a vertex (in which case we must take the lower limit of the sum over j to be -1), the β and α -terms thus generated exactly cancel the β and α -terms in figure 6. If $-\Lambda\partial_\Lambda|_\alpha$ strikes either an effective propagator or a gauge remainder, we adjust the ranges on the sums over m and j to remove any Wilsonian effective action one-point vertices. Having done this, we can increase the lower limit on s to remove certain diagrams which vanish at $\mathcal{O}(p^2)$. This works as follows. Suppose that $s = 0$ and that all diagrams with one-point vertices have been discarded. There are $2j + 4$ fields available to decorate the $j + 2$ vertices and so each vertex must be exactly two-point. However, recall from (10) that the $\mathcal{O}(p^2)$ part of all $n > 0$ loop, two-point vertices vanishes. As with diagrams possessing one-point vertices, it is useful to keep diagrams known to vanish at $\mathcal{O}(p^2)$ until after $-\Lambda\partial_\Lambda|_\alpha$ has acted. The resulting terms which individually possess $\mathcal{O}(p^2)$ components are all involved in diagrammatic cancellations.

Both a_0 and a_1 have the capacity to replace a one-point Wilsonian effective action vertex with something else. In the former case, a one-point Wilsonian effective action vertex is replaced by a dumbbell structure possessing a one-point vertex; the component of this structure in which the one-point vertex is a seed action vertex survives. In the latter case, a one-point, Wilsonian effective action vertex is replaced by a padlock structure which is decorated by a single field.

Now let us consider the effect of the action of a_1 in more detail. Due to the equivalence of each of the vertices in a given term, we can take the a_1 to strike the vertex with argument $v^{j+;R}$ (so long as we multiply by $j + 2$), causing the argument to become $\Sigma_{v^{j+;R}}$. The R has been dropped, since a quantum term is necessarily formed from a vertex whose argument is greater than zero. The lower limit on the sum over v^{j+} should now be changed from zero to one, in recognition of the fact that a_1 does not act on tree level terms. Furthermore, the sum over all vertex arguments is now $n + s - 1$, rather than $n + s$, and so we should reduce the upper limit of the sum over s by one. It is convenient to change variables:

$$\begin{aligned} v^{j+} &\rightarrow v^{j+} + 1 \\ v^j &\rightarrow v^j + 1 \\ &\vdots \end{aligned}$$

and then to let $s \rightarrow s - 1$.

The action of a_0 requires care since we must take the reduction of a vertex struck by a_0 seriously. This follows because terms formed by a_0 , unlike α -terms, β -terms or terms formed by a_1 , can be spawned by tree level vertices. Recall that a reduced vertex

lacks a two-point, tree level component. The flow of a reduced vertex must therefore lack a component given by the flow of a two-point, tree level vertex. It follows from (13) that the dumbbell structure generated by the flow of a reduced vertex either possesses at least one reduced vertex or the kernel is decorated. We denote the reduction of a dumbbell structure by tagging the structure with R . The terms generated by allowing $-\Lambda\partial_\Lambda|_\alpha$ to act in (19) are shown in figure 7.

$$\begin{aligned}
\mathcal{D}_n \rightarrow \mathcal{D}'_n & - \sum_{s=0}^n \sum_{m=0}^{2s+1} \sum_{j=-1}^{n+s-m-1} \frac{\Upsilon_{j+s+1,j+1}}{m!} \left[\begin{array}{c} \sum_{v^k=1}^{j+} \\ \text{D.1} \\ \textcircled{v^k} \\ \bullet \\ \textcircled{v^{j+,k}} \\ R \\ \textcircled{n_s, j} \end{array} \right]^{11\Delta^{j+s+1} > m} \\
& + \sum_{s=1}^n \sum_{m=0}^{2s-1} \sum_{j=-1}^{n+s-m-2} \frac{\Upsilon_{j+s,j+1}}{m!} \left[\begin{array}{c} \text{D.2} \\ \bullet \\ \textcircled{\Sigma_{v^{j+}}} \\ \textcircled{n_s, j} \end{array} \right]^{11\Delta^{j+s} > m} \\
& + \sum_{s=1}^n \sum_{m=0}^{2s} \sum_{j=-2}^{n+s-m-2} \frac{\Upsilon_{j+s,j+2}}{m!} \left[\begin{array}{c} \text{D.3} \\ \textcircled{v^{j+;R}} \\ \textcircled{n_s, j} \end{array} \right]^{11\Delta^{j+s} \overset{\bullet}{\Delta} > m} \\
& + 2 \sum_{s=1}^n \sum_{m=1}^{2s} \sum_{j=-2}^{n+s-m-2} \frac{\Upsilon_{j+s+1,j+2}}{(m-1)!} \left[\begin{array}{c} \text{D.4} \\ \textcircled{v^{j+;R}} \\ \textcircled{n_s, j} \end{array} \right]^{11\Delta^{j+s+1} > m-1 \overset{\bullet}{>}}
\end{aligned}$$

Figure 7. Expression for \mathcal{D}_n obtained by allowing $-\Lambda\partial_\Lambda|_\alpha$ to act in (19) and discarding terms which vanish at $\mathcal{O}(p^2)$ or possess a one-point, Wilsonian effective action vertex.

We now isolate all two-point, tree level vertices in diagram D.1. This step is crucial to the entire diagrammatic procedure: if a two-point, tree level vertex is attached to an effective propagator, we can employ the effective propagator relation, whereas if it is attached to an external field, we can perform manipulations at $\mathcal{O}(p^2)$.

Let us consider isolating the two-point, tree level vertices of diagram D.1 in more detail. First, let us take both vertices of the dumbbell structure to be reduced vertices. This immediately allows us to reduce the maximum value of the sum over j by one, since the total number of reduced vertices is now $j + 3$, rather than $j + 2$. Of the terms which remain, consider those possessing exclusively Wilsonian effective action vertices. Since we discard one-point, Wilsonian effective action vertices in all diagrams in which $\Lambda\partial_\Lambda|_\alpha$ has acted, we can reduce the maximum values of j and m and increase the minimum value of s by one. The component of the resulting diagram in which the kernel is undecorated is exactly cancelled by the component of diagram D.3 in which the differentiated effective propagator joins two different vertices. Since the surviving component has a decorated kernel, the maximum values of both m and j are reduced by one, again.

Isolating a single, two-point, tree level vertex in diagram D.1 is straightforward: taking the argument of the top or bottom vertex of the dumbbell structure to be a two-point, tree level vertex amounts to the same thing; hence we will choose to isolate the two-point, tree level part of \bar{v}^k and multiply by two. When taking the tree level part of \bar{v}^k , the other vertex argument, $\bar{v}^{j+,k;R} \equiv \bar{v}^{j+;R} - \bar{v}^{k;R}$, reduces to simply $\bar{v}^{j+;R}$. The equality of the two-point, tree level Wilsonian effective action vertices allows us to simplify the bar notation: from (12) only the seed action component of $\bar{v}^{j+;R}$ (which comes with a minus sign) survives. There is no need to change the limits on any of the sums: compared to the parent diagram, we have an extra two-point vertex, but also an extra two decorative fields, corresponding to the two ends of the kernel.

Taking two two-point, tree level vertices in diagram D.1 requires some thought. First, we note that by the definition of R acting on a dumbbell, the kernel must be decorated, which we indicate by the notation $\text{---}^\circ\text{---}$. Secondly, the dumbbell structure cannot have been formed by the flow of a one-point vertex. Since we are interested only in one-point Wilsonian effective action vertices if they have been processed, we can reduce the maximum values of m and j and increase the minimum value of s to remove any unwanted diagrams. If $j = -1$, then there are only two vertices in total, and so this case should be treated differently from $j \geq 0$. In the latter case, it will prove useful to shift variables $j \rightarrow j + 1$, so that the sum over j starts, once again, from -1 . The isolation of the two-point, tree level vertices of diagram D.1, together with the cancellation of the component of diagram D.3 in which the differentiated effective propagator joins two separate vertices, is shown in figure 8.

The next step of the diagrammatic procedure is to decorate the two-point, tree level vertices of diagrams D.6, D.8 and D.9, with either an external field or an end of an effective propagator. In the latter case we must then attach the loose end of any

$$\begin{aligned}
& - \sum_{s=1}^n \sum_{m=0}^{2s-1} \sum_{j=-1}^{n+s-m-4} \frac{\Upsilon_{j+s+1,j+1}}{m!} \sum_{v^k=1}^{v^{j+1}} \left[\begin{array}{c} \text{D.5} \\ \begin{array}{c} \textcircled{v^{k;R}} \\ | \\ \circ \\ | \\ \textcircled{v^{j+,k;R}} \end{array} \\ \textcircled{n_s, j} \end{array} \right]^{11\Delta^{j+s+1} > m} \\
& + \left[\begin{array}{c} \sum_{m=0}^{2n-1} \frac{\Upsilon_{n,0}}{m!} \\ \text{D.6} \\ \begin{array}{c} \textcircled{0^2} \\ | \\ \circ \\ | \\ \textcircled{0^2} \end{array} \end{array} \right]^{11\Delta^n > m} + 2 \sum_{v^k=1}^{v^{j+1}} \left[\begin{array}{c} \sum_{s=0}^n \sum_{m=0}^{2s+1} \sum_{j=-1}^{n+s-m-2} \frac{\Upsilon_{j+s+1,j+1}}{m!} \\ \text{D.7} \\ \begin{array}{c} \textcircled{\hat{v}^{k;R}} \\ | \\ \bullet \\ | \\ \textcircled{v^{j+,k;R}} \end{array} \\ \textcircled{n_s, j} \end{array} \right]^{11\Delta^{j+s+1} > m} \\
& + \left[\begin{array}{c} \sum_{s=1}^n \sum_{m=0}^{2s-1} \sum_{j=-1}^{n+s-m-3} \frac{\Upsilon_{j+s+2,j+2}}{m!} \\ \text{D.8} \\ \begin{array}{c} \textcircled{0^2} \\ | \\ \circ \\ | \\ \textcircled{0^2} \\ | \\ \textcircled{v^{j+,R}} \\ | \\ \textcircled{n_s, j} \end{array} \end{array} \right]^{11\Delta^{j+s+2} > m} + 2 \left[\begin{array}{c} \sum_{s=0}^n \sum_{m=0}^{2s+1} \sum_{j=-1}^{n+s-m-1} \frac{\Upsilon_{j+s+1,j+1}}{m!} \\ \text{D.9} \\ \begin{array}{c} \textcircled{0^2} \\ | \\ \bullet \\ | \\ \textcircled{\hat{v}^{j+,R}} \\ | \\ \textcircled{n_s, j} \end{array} \end{array} \right]^{11\Delta^{j+s+1} > m}
\end{aligned}$$

Figure 8. Isolation of the two-point, tree level vertices of diagram D.1. The effect of cancelling the component of diagram D.3 in which the differentiated effective propagator joins two separate vertices forces the kernel of diagram D.5 to possess only decorated components.

effective propagators to an available structure. We refer to the primary part of such a diagram as the component left over after applying the effective propagator relation as many times as possible but, each time, retaining only the Kronecker- δ contribution.

Assuming that the necessary structures exist, we can do the following with a diagram possessing a single two-point, tree level vertex:

- (i) attach an external field;
- (ii) attach one end of an effective propagator, with the other end attaching to:

- (a) one of the Wilsonian effective action vertices;
- (b) the seed action vertex to which the kernel attaches;
- (c) the kernel;
- (d) a gauge remainder.

In each of (ii)a–(ii)d the effective propagator relation can be applied. For the purposes of this paper, we will concern ourselves with just the primary part coming from (ii)a and (ii)b; the treatment of the gauge remainder contributions and (ii)d is deferred until [16].||;

Cancellation 1 (Diagram D.7) *Consider the primary part of diagram D.9 corresponding to (ii)a, above, which we note exists only for $j > -1$. For comparison with diagram D.7, it is convenient to change variables $j \rightarrow j + 1$, so that the sum over j once again starts from -1 and to identify \hat{v}^{j+2} with \hat{v}^k . Thus, the two-point, tree level vertex can be joined to any of $j + 2$ identical Wilsonian effective action vertices, using any of $j + s + 2$ effective propagators. Noting that this effective propagator can attach either way round, the combinatoric factor is*

$$2(j + s + 2)(j + 2),$$

which, from (20), combines with $\Upsilon_{j+s+2,j+2}$ to give $-\Upsilon_{j+s+1,j+1}$. Thus, the primary part of diagram D.9 corresponding to (ii)a, above, precisely cancels diagram D.7.

Before discussing cancellations arising from the primary part of diagram D.9 corresponding to (ii)b, we consider a cancellation arising from one of the diagrams possessing two two-point vertices.

Cancellation 2 (Diagram D.5) *Consider attaching each two-point, tree level vertex of diagram D.8 to a separate reduced vertex. The primary part of this diagram precisely cancels diagram D.5.*

Similarly, it is straightforward to show that all components of diagram D.2 are cancelled by the following terms:

- (i) The component of diagram D.3 in which the differentiated effective propagator attaches at both ends to the same vertex;
- (ii) The primary part of diagram D.9 corresponding to (ii)b, above;
- (iii) The primary part of diagram D.8 in which both two-point, tree level vertices are attached to the same reduced vertex;
- (iv) The primary parts of diagrams D.6 and D.8 in which the two-point, tree level vertices are attached to each other.

We have thus demonstrated that, up to terms involving gauge remainders or possessing an $\mathcal{O}(p^2)$ stub, \mathcal{D}_n does indeed vanish at $\mathcal{O}(p^4)$. The complete proof, to

|| The primary part coming from (ii)c corresponds to a kernel which bites its own tail, and so can be discarded.

be given in [16], is considerably more arduous than the partial demonstration given here, requiring further diagrammatic techniques. However, given that \mathcal{D}_n does vanish at $\mathcal{O}(p^4)$ we can then directly derive an expression for β_n in terms of just Wilsonian effective action vertices, effective propagators and (components of) gauge remainders. First, we specialize \mathcal{D}_n to $\mathcal{O}(p^2)$ and so discard all terms which are manifestly $\mathcal{O}(p^4)$. Then we notice that the only remaining term containing β_n multiplies a two-point, tree level vertex. However, from (9), the $\mathcal{O}(p^2)$ part of this vertex is just a universal coefficient. Pulling the β_n term to the other side of the equation, we have an expression for β_n in terms of Wilsonian effective action vertices, effective propagators, (components of) gauge remainders and $\beta_{m<n}$. These latter terms can be substituted for using the diagrammatic expression for $\beta_{m<n}$ and so forth, until all β terms have been re-expressed diagrammatically.

References

- [1] J. I. Latorre and T. R. Morris, *JHEP* 0011 (2000) 004, [arXiv:hep-th/0008123].
- [2] S. Arnone, T. R. Morris and O. J. Rosten, [arXiv:hep-th/0507154].
- [3] T. R. Morris, in *The Exact Renormalization Group*, Eds. Krasnitz *et al* , World Sci (1999) 1, [arXiv:hep-th/9810104].
- [4] T. R. Morris, *Nucl. Phys.* **B 573** (2000) 97, [arXiv:hep-th/9910058].
- [5] T. R. Morris, *JHEP* 0012 (2000) 012, [arXiv:hep-th/0006064].
- [6] S. Arnone, A. Gatti and T. R. Morris, *Phys. Rev.* **D 67** (2003) 085003, [arXiv:hep-th/0209162].
- [7] O. J. Rosten, T. R. Morris and S. Arnone, Proceedings of Quarks 2004, Pushkinskie Gory, Russia, 24-30 May 2004, <http://quarks.inr.ac.ru>, [arXiv:hep-th/0409042].
- [8] O. J. Rosten, ‘The Manifestly Gauge Invariant Exact Renormalisation Group’, Ph.D. Thesis, [arXiv:hep-th/0506162].
- [9] O. J. Rosten, [arXiv:hep-th/0507166].
- [10] T. R. Morris and O. J. Rosten, [arXiv:hep-th/0508026].
- [11] S. Arnone, Y. A. Kubyshin, T. R. Morris and J. F. Tighe, *Int. J. Mod. Phys.* **A 17** (2002) 2283, [arXiv:hep-th/0106258].
- [12] S. Arnone, A. Gatti and T. R. Morris, *JHEP* 0205 (2002) 059, [arXiv:hep-th/0201237].
- [13] S. Arnone, A. Gatti, T. R. Morris and O. J. Rosten, *Phys. Rev.* **D 69** (2004) 065009, [arXiv:hep-th/0309242].
- [14] S. Arnone, T. R. Morris and O. J. Rosten, [arXiv:hep-th/0505169].
- [15] See e.g. S. Weinberg, *The Quantum Theory of Fields* (Cambridge University Press, Cambridge 1996), Vol. 2.
- [16] O. J. Rosten, In preparation.
- [17] Work in progress.
- [18] M. Bonini *et al* , *Nucl. Phys.* **B 409** (1993) 441.
- [19] M. Bonini, G. Marchesini and M. Simionato, *Nucl. Phys.* **B 483** (1997) 475.
- [20] T. R. Morris and J. F. Tighe, *JHEP* 9908 (1999) 007 [arXiv:hep-th/9906166].
- [21] T. Papenbrock and C. Wetterich, *Z. Phys.* **C 65** (1995) 519.
- [22] M. Pernici and M. Raciti, *Nucl. Phys.* **B 531** (1998) 560.
- [23] P. Kopietz, *Nucl. Phys.* **B 595** (2001) 493.
- [24] D. Zappala, *Phys. Rev.* **D 66** (2002) 105020.